Atmos. Meas. Tech. Discuss., 6, 3317–3338, 2013
www.atmos-meas-tech-discuss.net/6/3317/2013/
doi:10.5194/amtd-6-3317-2013

Atmospheric Measurement Techniques
Discussions
Open Access

Discussion Paper | Discussion Paper | Discussion Paper | Discussion Paper |

Retrieval of aerosol single scattering albedo and polarized phase function from polarized sun-photometer measurements for Zanjan atmosphere

A. Bayat[1], H. R. Khalesifard[1,2], and A. Masoumi[1]

[1]Department of Physics, Institute for Advanced Studies in Basic Sciences (IASBS), Zanjan 45137-66731, Iran
[2]Center for Climate Change and Global Warming, Institute for Advanced Studies in Basic Sciences (IASBS), Zanjan 45137-66731, Iran

Received: 14 March 2013 – Accepted: 20 March 2013 – Published: 4 April 2013

Correspondence to: A. Bayat (a_bayat@iasbs.ac.ir)

Published by Copernicus Publications on behalf of the European Geosciences Union.

Abstract

Aerosol optical depth, Ångström exponent, single scattering albedo, and polarized phase function have been retrieved from polarized sun-photometer measurements for atmosphere of Zanjan (36.70° N, 48.51° E, and 1800 m a.m.s.l.) from January 2010 to December 2012. The results show that the maximum value of aerosol polarized phase function as well as the polarized phase function retrieved for a specific scattering angle (i.e. 60°), are strongly correlated with the Ångström exponent. The latter one has a meaningful variations respect to the changes in the complex refractive index of the atmospheric aerosols. Furthermore the polarized phase function shows a moderate negative correlation respect to atmospheric aerosol optical depth and single scattering albedo. Therefore the polarized phase function can be regarded as a key parameter to characterize the atmospheric particles.

1 Introduction

Physical and optical properties of the atmospheric aerosols are from the major uncertainties in the global climate changes (Solomon et al., 2007). In order to reduce the lack of extensive and reliable information about aerosols and their impact on atmosphere, they have been widely investigated by ground-based measurements and satellite remote sensing suits (Heintzenberg et al., 1997; Kaufman et al., 2002). Ground-based measurements are ideal for reliable and continuous derivation of aerosol optical and physical properties due to negligible effects of surface background on the measurements (Holben et al., 1998; Dubovik et al., 2002).

Iran is located within the so-called Earth's dust belt. Many cities in west, east, south, and central part of this country had been subjected to dust events of different strength, especially during the recent years. Previous observations show that the Tigris–Euphrates Basin in west, Arabian Peninsula in south and southwest, and the arid region between the Caspian and Aral seas in north are the main external

AMTD
6, 3317–3338, 2013

sources for the observed dust activities in this region (Prospero et al., 2002; Leon and Legrand, 2003; Goudie et al., 2006; Bayat et al., 2011; Abdi et al., 2011, 2012; Sabetghadam et al., 2012; Masoumi et al., 2013). There are also some minor active dust sources inside the Iran plateau (Abdi et al., 2011, 2012; Masoumi et al., 2013). Zanjan, a city in Northwest Iran, is located in a mountainous region at 36.70° N, 48.51° E, and 1800 m a.m.s.l.. Zanjan meteorological office data shows that the average of sunny times for this city is more than 7 h per day (Samimi et al., 1997). Considering the geographical location as well as the climatological conditions and lack of measurement data for the region, ground based measurements in this city provide valuable information on the dust activities.

In our previous works, different optical and physical parameters of atmospheric aerosols including; aerosol optical depth (τ_a), Ångström exponent (α), volume size distribution, complex refractive index, and single scattering albedo (ω_0) have been studied during 2006 to 2010 (Bayat et al., 2011; Masoumi et al., 2013). In this work, both non-polarimetric and polarimetric measurements of a CIMEL CE318-2 sun-photometer (SPM) at 870 nm have been used to retrieve ω_0 and polarized phase function ($q_a(\Theta)$) of the aerosols. These parameters have been retrieved from recordings of sun-scattered radiance measurements at 870 nm in the Solar Principal Plane (SPP), during January 2010 to December 2012. The SPP is a sweep of sky in a plane that includes the sun and the zenith directions. Polarized sky radiance strongly depends on the presence of aerosols in the atmosphere and it can be monitored by looking through $q_a(\Theta)$ (Vermeulen et al., 2000). To characterize the atmospheric aerosols, we looked to the correlation between $q_a(\Theta)$ and α as well as $q_a(\Theta)$ and τ_a. Also the correlation between $q_a(\Theta)$ and ω_0 has been considered. It should be added that taking into account the aerosol polarized phase function inside the inversion algorithms that usually are used for retrieving the physical properties of the aerosols (i.e. aerosol volume size distribution and complex refractive index), increases the accuracy of calculations and outputs of the algorithms (Li et al., 2006).

AMTD
6, 3317–3338, 2013

The rest of manuscript is organized as follows: in Sect. 2, the retrieval algorithm of aerosol parameters has been explained. The measurement procedure and the obtained results are appeared in Sect. 3. Section 4 is a discussion over the obtained results.

2 Method

Propagation of solar radiation throughout the atmosphere can be modelled by solving the vector radiative transfer equation (VRTE) for a multilayer plane parallel atmosphere, where each layer is specified by its optical depth, single scattering albedo, and scattering matrix (Chandrasekhar, 1950; Zdunkowski et al., 2007). For a random distribution of spherical particles, the stokes vector of scattered light can be obtained by transferring its components for the incident light by means of:

$$\begin{pmatrix} I_s \\ Q_s \\ U_s \\ V_s \end{pmatrix} = \frac{\Omega_{\text{eff}}}{4\pi} \begin{pmatrix} P_{11}(\Theta) & P_{12}(\Theta) & 0 & 0 \\ P_{12}(\Theta) & P_{22}(\Theta) & 0 & 0 \\ 0 & 0 & P_{33}(\Theta) & P_{34}(\Theta) \\ 0 & 0 & -P_{34}(\Theta) & P_{44}(\Theta) \end{pmatrix} \begin{pmatrix} I_0 \\ 0 \\ 0 \\ 0 \end{pmatrix}, \tag{1}$$

where Θ is the scattering angle, Ω_{eff} indicates the effective solid angle associated with the scattering angle and can be obtained by normalization of the phase function, $p_a(\Theta)$ [i.e. the $P_{11}(\Theta)$ term] (Van de Hulst, 1980; Zdunkowski et al., 2007). Here, the aerosol polarized phase function, $q_a(\Theta)$, stands for the $P_{12}(\Theta)$ term. I, Q, U, and V are the stokes parameters, and the subscript "s" refers to the scattered light. Since the incident solar light at the top of the atmosphere is unpolarized, its Stokes parameters would be represented by [I_0, 0, 0, 0]. On the ground level the total sky radiance and polarized sky radiance (L and L_p) respectively equals to I_s and Q_s, that can be extracted from the total and polarized measurements of the SPM in the SPP mode (Vermeulen et al., 2000; Li et al., 2007, 2009).

AMTD
6, 3317–3338, 2013

The total and polarized sky radiance in the SPP measurement mode have been estimated by solving the VRTE by using the successive order of scattering method (Siewert, 1982; Deuzé et al., 1989; Dubovik et al., 2000; Lenoble et al., 2007; Zdunkowski et al., 2007). Table 1 shows the required parameters that should be used in VRTE to estimate the L and L_p. Also, the corresponding measurement or retrieval technique for each parameter has been presented in Table 1.

Using the obtained L and L_p one may retrieve ω_0, $p_a(\Theta)$, and $q_a(\Theta)$ (Devaux et al., 1998; Vermeulen et al., 2000). For simplicity from now on we remove the argument Θ and write $p_a(\Theta)$, and $q_a(\Theta)$ just as p_a, and q_a. In this method the contribution of ground reflectance, molecular scattering, and aerosol multiple scattering have been eliminated from the measurements to retrieve the single scattering properties of the atmospheric aerosols (Vermeulen et al., 2000). Since the ratio of (single scattering)/(total scattering) of the sky radiance is nearly the same for measurements and calculations, the relationship between the actual and estimated (marked with a superscript *) sky radiance is given by

$$\frac{\omega_0}{\omega_0^*} p_a = \frac{L-(L^*-L_0^*)}{L_0{}^*} p_a^* + \frac{L-L^*}{L_0{}^*} \frac{\tau_m}{\omega_0^* \tau_a} p_m, \tag{2}$$

where L is the measured, and L^* the estimated total sky radiance. L_0^*, p_a^*, p_m, and τ_m are the estimated sky radiance in the absence of ground reflection, the estimated aerosol phase function, the molecular phase function, and the molecular optical depth respectively (Vermeulen et al., 2000). Considering the normalization condition for p_a, i.e.

$$\int_0^\pi \omega_0 p_a \sin\Theta d\Theta = 2\omega_0, \tag{3}$$

AMTD
6, 3317–3338, 2013

Polarized sun-photometer measurements for Zanjan atmosphere

A. Bayat et al.

and Eq. (2), will lead to

$$\frac{2\omega_0}{\omega_0^*} = \int_0^{\pi} \left(\frac{L-(L^*-L_0^*)}{L_0^*} p_a^* + \frac{L-L^*}{L_0^*} \frac{\tau_m}{\omega_0^* \tau_a} p_m\right) \sin\Theta d\Theta, \tag{4}$$

where Θ is the scattering angle. The right-hand side of Eq. (4) has been calculated for ω_0^* =0.6, 0.7, 0.8, 0.9, and 1.0, then an interpolation has been applied to obtained values to converge the value of the integral to 2, that leads to $\omega_0^* = \omega_0$ in the left hand side. Replacing the retrieved value of ω_0 in Eq. (2), the measured aerosol phase function can be retrieved as

$$p_a = \frac{L-(L^*(\omega_0)-L_0^*(\omega_0))}{L_0^*(\omega_0)} p_a^* + \frac{L-L^*(\omega_0)}{L_0^*(\omega_0)} \frac{\tau_m}{\omega_0 \tau_a} p_m. \tag{5}$$

In the same way q_a can be written as

$$q_a = \frac{L_p}{L_p^*(\omega_0)} q_a^* + \frac{L_p-L_p^*(\omega_0)}{L_p^*(\omega_0)} \frac{\tau_m}{\omega_0 \tau_a} q_m, \tag{6}$$

where q_a^* is the estimated polarized phase function, and q_m is the molecular polarized phase function (Vermeulen et al., 2000). Already it has been shown that for a calibrated CIMEL SPM the accuracy on τ_a(870 nm) is ±0.01, and the estimated total error of the retrieved ω_0 at 870 nm is about ±0.05. The accuracy of q_a at 870 nm when $20^\circ < \Theta < 120^\circ$ is about 10 % (Holben et al., 1998; Devaux et al., 1998; Vermeulen et al., 2000; Li et al., 2006).

During the retrieval of the above mentioned parameters, most of the cloud contaminated data has been eliminated via using the Aerosol Robotic Network (AERONET) cloud screening algorithm (Smirnov et al., 2000). After applying the screening algorithm, still some contaminations were over the data due to existence of inhomogeneous scattered clouds. These have been identified and removed by fitting a robust locally weighted regression to the radiance measurements in the SPP mode (Li et al., 2004). After applying the above procedure, totally 305 measurements have been selected.

3 Measurements and results

In this work, we have investigated the data recorded by a polarized SPM (CIMEL CE318-2) during a 26-month period, as mentioned in Introduction section. The SPM is registered as IASBS on the AERONET and has been calibrated under protocols of the network for the mentioned period. It should be added, during 9 October 2010 to 2 March 2011, and 18 January 2012 to 3 August 2012, the SPM has been sent for calibration [1]. τ_a at four wavelengths (440, 675, 870, and 1020 nm) and α (calculated for τ_a at 440, 675, and 870 nm) have been retrieved from the sun mode recorded data (Holben et al., 1998; Toledano et al., 2007; Bayat et al., 2011). Total and polarized sky radiance at 870 nm have been obtained from the SPP recordings to retrieve the ϖ_0 and q_a (Devaux et al., 1998; Vermeulen et al., 2000).

Figure 1a–d shows the temporal variations of the retrieved τ_a(870 nm), α, q_a(max), and ϖ_0 for the atmosphere of Zanjan and Table 2 includes their minimum, maximum, and mean values for the measurement period. Here q_a(max) stands for the maximum value of q_a. Figure 1b, d and Table 2 illustrate that both absorptive fine aerosols (smaller ϖ_0 and $\alpha > 0.7$) and non-absorptive coarse ones (larger ϖ_0 and $\alpha < 0.7$) are presented in the atmosphere of Zanjan with a larger share of the latter ones. Such behavior is due to dominant existence of dust particles especially in late spring and early summer while almost a constant background contamination of anthropogenic aerosols exists in the atmosphere. This is quite in agreement with our previous results that indicate dust is the main contaminant of the atmosphere in this region (Bayat et al., 2011; Masoumi et al., 2013). Figure 1d includes ϖ_0 values from AERONET that have been retrieved from the almucantar sky recordings at 870 nm for IASBS site as well as its values that have been obtained from SPP measurement recordings (our technique). The accuracy of retrieved ϖ_0 from AERONET is ~ 0.03 to ~ 0.07 (Dubovik et al., 2002). The retrieved

[1] The calibrations have been carried in the Photon Group, Laboratoire d'Optique Atmosphérique (LOA) – UFR de Physique Université des Sciences et Technologies de Lille (USTL) – CNRS.

AMTD
6, 3317–3338, 2013

ω_0 accuracy from the both mentioned algorithms depend on τ_a, i.e. the larger τ_a the better accuracy. Referring to Fig. 1d, the difference between the results obtained from the two mentioned techniques is less than 0.05 for most of the cases. The differences also can be due to the time difference of about 10 min between these two measurement modes and also to the different impact of the surface reflectance on their measurement geometries. Referring to Fig. 1b, c, it can be observed, α and q_a(max) more or less have similar temporal variations. In other words, it can be concluded that q_a(max) is more sensitive to the aerosol size respect to other parameters, i.e. τ_a and ω_0.

Figure 2 depicts variations of q_a versus the scattering angle for two measurements with the same τ_a but different α. The larger (smaller) $\alpha = 1.49$ ($\alpha = 0.78$) corresponds to the larger (smaller) value of $q_a(\max) = 0.22$ ($q_a(\max) = 0.09$).

Figure 2 is an example of such comparisons and other measurements also show similar behaviors. This can be observed in Fig. 3 where there is a strong positive correlation between q_a(max) and α. The color bar in Fig. 3 corresponds to τ_a values in logarithmic scale. As in our previous work (Masoumi et al., 2013) a negative correlation between α and τ_a can be observed in Fig. 3.

In Fig. 4, variations of q_a at different scattering angles have been compared for atmospheres with the same α but different τ_a. These results illustrate a moderate influence of variations of τ_a on q_a. Figure 5 depicts the variations of q_a(max) at different values of τ_a. Colors in this figure are mapped to different values of α in linear scales. By looking to Fig. 5, one can conclude that q_a is not so much sensitive respect to τ_a and has a moderate negative correlation with its variations.

4 Discussion

Our previous works, showed that dust and anthropogenic aerosols are the most dominant contaminant particles in the Zanjan atmosphere (Bayat et al., 2011; Masoumi et al., 2013). Considering the positive and negative correlations of q_a(max) with α and τ_a, respectively (Figs. 3 and 5), one may conclude, during dust activities (increase

AMTD
6, 3317–3338, 2013

of aerosol size and τ_a), q_a(max) considerably is decreasing. A comparison between Figs. 3 and 5 shows that q_a(max) is more sensitive to α than τ_a for this region. As mentioned before, ϖ_0 is another crucial parameter in characterization of atmospheric aerosols. It mostly depends on the particles composition and size distribution (Dubovik et al., 2002). Figure 6 shows the correlation between q_a(max) and ϖ_0, where colors indicate for variations of τ_a. Each data point has been specified by a solid circle whose diameter is mapped to α^{-1} as a qualitative measure of the particle size. For $\tau_a > 0.30$, q_a(max) is almost constant (~ 0.05). Also, a moderate negative correlation between q_a(max) and ϖ_0 can be observed, when τ_a is less than 0.30. As a result, the smaller and absorptive aerosols (smaller value of ϖ_0 when $\tau_a < 0.30$) in the atmosphere cause the larger polarized phase function, and vice versa. Therefore, the polarized phase function can be chosen as a good candidate to characterize the atmospheric particles. To check this, in Fig. 7, $q_a(60^\circ)$ has been plotted versus α for three different refractive indices ($m_1 = 1.40 - i0.010$, $m_2 = 1.45 - i0.005$, and $m_3 = 1.55 - i0.001$), based on the Mie scattering theory for spherical particle. The plots have been overlaid on the retrieved values $q_a(60^\circ)$ for the measurements in the IASBS site. The chosen refractive indices m_1, m_2, and m_3, are almost corresponding to anthropogenic aerosols (Dubovik et al., 2002), Southeast Asian aerosols (AERONET network, Chen-Kung site in Taiwan), and dust (Dubovik et al., 2002) respectively. Figure 7 shows, the events with lower values of α are almost close to the curve for m_3 (dust) but as α increases the data get more close to m_2 and m_1 curves that are corresponding to the aerosols resulted from incomplete fuel burning and anthropogenic aerosols respectively (Dubovik et al., 2002; Cattrall et al., 2005; Kokhanovsky, 2008). The figure also shows that for $\alpha < 0.4$, the data is not well fitted to the curves. We guess this should be due to the spherical shape assumption for the particles in retrieving q_a. Finally we would like to conclude, the polarized phase function is a powerful tool for characterizing the atmospheric aerosols and can provide valuable information on their optical and physical properties.

AMTD
6, 3317–3338, 2013

Acknowledgements. Authors would like to express their gratitude to the AERONET team for preparing Almucantar measurements parameters in the network.

References

Abdi, F., Flamant, C., Cuesta, J., Flamant, P., and Khalesifard, H. R.: Multiplatform observations of dust vertical distribution during transport over northwest Iran in the summertime, J. Geophys. Res., 116, D05206, doi:10.1029/2010JD014573, 2011. 3319

Abdi, F., Flamant, C., Cuesta, J., Oolman, L., Flamant, P., and Khalesifard, H. R.: Dust transport over Iraq and northwest Iran associated with winter Shamal: a case study, J. Geophys. Res., 117, D03201, doi:10.1029/2011JD016339, 2012. 3319

Bayat, A., Masoumi, A., and Khalesifard, H. R.: Retrieval of atmospheric optical parameters from ground-based sun-photometer measurements for Zanjan, Iran, Atmos. Meas. Tech., 4, 857–863, doi:10.5194/amt-4-857-2011, 2011. 3319, 3323, 3324

Bodhaine, B. A., Wood, N. B., Dutton, E. G., and Slusser, J. R.: On Rayleigh optical depth calculations, J. Atmos. Ocean. Tech., 16, 1854–1861, 1999. 3330

Cattrall, C., Reagan, J., Thome, K., and Dubovik, O.: Variability of aerosol and spectral lidar and backscatter and extinction ratios of key aerosol types derived from selected Aerosol Robotic Network locations, J. Geophys. Res., 110, D10S11, doi:10.1029/2004JD005124, 2005. 3325

Chandrasekhar, S.: Radiative Transfer, Oxford University Press, Oxford, 1950. 3320

Deuzé, J. L., Herman, M., and Santer, R.: Fourier series expansion of the transfer equation in the atmosphere–ocean system, J. Quant. Spectrosc. Ra., 41, 483–494, 1989. 3321

Devaux, C., Vermeulen A., Deuzé, J. L., Dubuisson, P., Herman, M., Santer, R., and Verbrugghe, M.: Retrieval of aerosol single scattering albedo from ground-based measurements: application to observational data, J. Geophys. Res., 103, 8753–8761, 1998. 3321, 3322, 3323

Dubovik, O. and King, M. D.: A flexible inversion algorithm for retrieval of aerosol optical properties from sun and sky radiance measurements, J. Geophys. Res., 105, 20673–20696, 2000. 3321

Dubovik, O., Holben, B. N., Eck, T. F., Smirnov, A., Kaufman, Y. J., King, M. D., Tanré, D., and Slutsker, I.: Variability of absorption and optical properties of key aerosol types observed in worldwide locations, J. Atmos. Sci., 59, 590–608, 2002. 3318, 3323, 3325

Goudie, A. S. and Middleton, N.: Desert Dust in the Global System, Springer Press, Heidelberg, 2006. 3319

Heintzenberg, J., Charlson, R. J., Clarke, A. D., Liousse, C., Ramaswamy, V., Shine, K. P., Wendisch, M., and Helas, G.: Measurements and modeling of aerosol single scattering albedo: progress, problems and prospects, Beitr. Phys. Atmos., 70, 249–263, 1997. 3318

Holben, B. N., Eck, T. F., Slutsker, I., Tanre, D., Buis, J. P., Setzer, A., Vermote, E., Reagan, J. A., Kaufman, Y. J., Nakajima, T., Lavenu, F., Jankowiak, I., and Smirnov, A. : AERONET – a federated instrument network and data archive for aerosol characterization, Remote Sens. Environ., 66, 1–16, 1998. 3318, 3322, 3323, 3330

Kaufman, Y. J., Tanré, D., and Boucher, O.: A satellite view of aerosols in the climate system, Nature, 418, 215–223, 2002. 3318

Kokhanovsky, A. A.: Aerosol Optics, Light Absorption and Scattering by Particles in the Atmosphere, Springer-Praxis Press, Chichester, UK, 2008. 3325

Lenoble, J., Herman, M., Deuzé, J. L., Lafrance, B., Santer, R., and Tanré, D.: A successive order of scattering code for solving the vector equation of transfer in the earth's atmosphere with aerosols, J. Quant. Spectrosc. Ra., 107, 479–507, 2007. 3321

Leon, J. and Legrand, M.: Mineral dust sources in the surrounding of the North Indian Ocean, Geophys. Res. Lett., 30, 1309, doi:10.1029/2002GL016690, 2003. 3319

Li, Z., Goloub, P., Devaux, C., Gu, X., Qiao, Y., Zhao, F., and Chene, H.: Aerosol polarized phase function and single-scattering albedo retrieved from groundbased measurements, Atmos. Res., 71, 233–241, 2004. 3322

Li, Z., Goloub, P., Devaux, C., Gu, X., Qiao, Y., and Zhao, F.: Retrieval of aerosol optical and physical properties from groundbased spectral, multi-angular and polarized sun-photometer measurements, Remote Sens. Environ., 101, 519–533, 2006. 3319, 3322

Li, Z., Goloub, P., Blarel, L., Damiri, B., Podvin, T., and Jankowiak, I.: Dust optical properties retrieved from ground-based polarimetric measurements, Appl. Optics, 46, 1548–1553, 2007. 3320

Li, Z., Goloub, P., Dubovik, O., Blarel, L., Zhang, W., Podvin, T., Sinyuk, A., Sorokin, M., Chen, H., Holben, B., Tanré, D., Canini, M., and Buis, J.-P.: Improvements for ground-based remote sensing of atmospheric aerosol properties by additional polarimetric measurements, J. Quant. Spectrosc. Ra., 110, 1954–1961, 2009. 3320

Liou, K. N.: An Introduction to Atmospheric Radiation, Academic Press, San Diego, CA, 2002. 3330

AMTD

6, 3317–3338, 2013

Polarized sun-photometer measurements for Zanjan atmosphere

A. Bayat et al.

Lucht, W. and Roujean, J. L.: Consideration in parametric modeling of BRDF and albedo from multi-angular satellite sensors observations, Remote Sens. Rev., 18, 343–379, 2000. 3330

Masoumi A., Khalesifard H. R., Bayat A., and Moradhaseli R.: Retrieval of aerosol optical and physical properties from ground-based measurements for Zanjan, a city in Northwest Iran, Atmos. Res., 120–121, 343–355, 2013. 3319, 3323, 3324

Michalsky, J. J.: The astronomical Almanac's algorithm for approximate solar position (1950–2050), Sol. Energy, 40, 227–235, 1988. 3330

Prospero, J. M., Ginoux, P., Torres, O., Nicholson, S. E., and Gill, T. E.: Environmental characterization of global sources of atmospheric soil dust identified with the NIMBUS 7 Total Ozone Mapping Spectrometer (TOMS) absorbing aerosol product, Rev. Geophys., 40, 1002–1029, 2002. 3319

Sabetghadam, S., Ahmadi-Givi, F., and Golestani, Y.: Visibility trends in Tehran during 1958–2008, Atmos. Environ., 62, 512–520, 2012. 3319

Samimi, J. and Anvari, A.: Envestigation and Analysis of Solar Energy Information and its Potantioal in Iran, Tech. Report, Center for Energy Studies, Iran, Ministry of energy, Iran, 1997. 3319

Siewert C. E.: On the phase matrix basic to the scattering of polarized light, Astron. Astrophys., 109, 195–200, 1982. 3321

Smirnov, A., Holben, B. N., Eck, T. F., Dubovik, O., and Slutsker, I.: Cloud Screening and quality control algorithms for the AERONET database, Remote Sens. Environ., 73, 337–349, 2000. 3322

Solomon, S., Qin, D., Manning, M., Chen, Z., Marquis, M., Averyt, K. B., Tignor, M., and Miller, H. L. (Eds.): IPCC. Climate Change 2007: The Physical Science Basis. Contribution of Working Group I to the Fourth Assessment Report of the Intergovernmental Panel on Climate Change, Cambridge University Press, Cambridge, UK and New York, NY, USA, 996 pp., 2007. 3318

Toledano, C., Cachorro, V. E., Berjon, A., de Frutos, A. M., Sorribas, M., de la Morena, B. A., and Goloub, P.: Aerosol optical depth and Ångström exponent climatology at “El Arenosillo” AERONET site (Huelva, Spain), Q. J. Roy. Meteor. Soc., 133, 795–807, 2007. 3323, 3330

Van de Hulst, H. C.: Multiple Light Scattering. Tables, Formulas, and Applications, 2 Volumes, Academic Press, New York, 1980. 3320

AMTD

6, 3317–3338, 2013

Polarized sun-photometer measurements for Zanjan atmosphere

A. Bayat et al.

Vermeulen, A., Devaux, C., and Herman, M.: Retrieval of the scattering and microphysical properties of aerosols from groundbased optical measurements including polarization: I. Method, Appl. Optics, 39, 6207–6220, 2000. 3319, 3320, 3321, 3322, 3323
Zdunkowski, W., Trautmann, T., and Bott, A.: Radiation in the Atmosphere. A course in Theoretical Meteorology, Cambridge University Press, New York, 2007. 3320, 3321

Table 1. The required parameters for solving VRTE to calculate the L and L_p.

Parameter	Measurement or retrieval technique	Referance
τ_a(870 nm)	Sun mode recordings	Holben et al. (1998)
α	Retrieved from τ_a at 440, 675, 870 nm	Toledano et al. (2007)
τ_m	Surface pressure recorded data From on site weather station (CIMEL, Model: ENERCO 408p)	Bodhaine et al. (1999)
Solar-zenith angle	Astronomical Almanac's algorithm	Michalsky (1988)
Ground surface reflectance	MODIS surface reflectance product	Lucht et al. (2000)
Molecular scattering matrix	Rayleigh scattering theory	Liou (2002)
Aerosol scattering matrix	Mie scattering theory	Liou (2002)
ϖ_0	Mie scattering theory	Liou (2002)

AMTD
6, 3317–3338, 2013

Table 2. Minimum, maximum, and mean values of τ_a, α, q_a(max), and ϖ_0 for 305 selected data, January 2010 to December 2012, IASBS site.

	Min	Max	Mean
τ_a	0.02	0.61	0.15
α	0.07	1.79	0.85
q_a(max)	0.04	0.32	0.14
ϖ_0	0.64	0.99	0.90

AMTD
6, 3317–3338, 2013

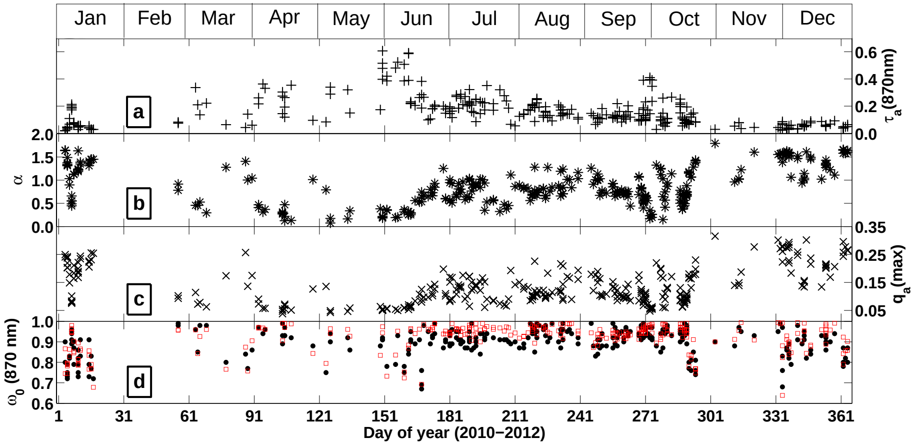

Fig. 1. (a) τ_a(870 nm), **(b)** α, **(c)** q_a(max), and **(d)** ϖ_0 retrieved from SPP mode (our results, solid black circles) and Almucantar mode (AERONET results, empty red squares) measurements versus day of year, January 2010 to December 2012, IASBS site.

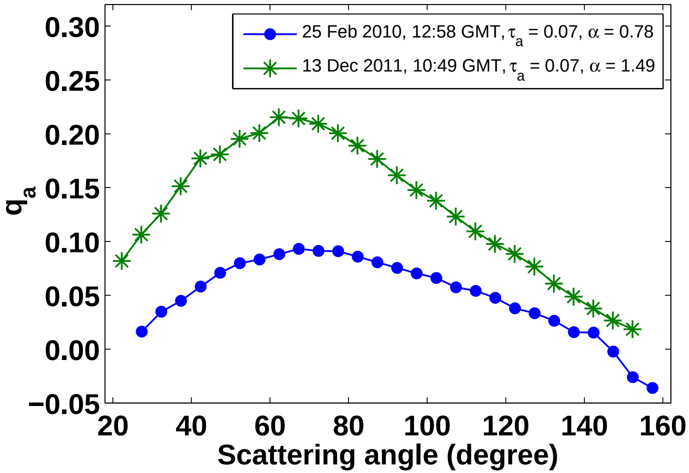

Fig. 2. Retrieved q_a at 870 nm versus the scattering angle, in the atmosphere of Zanjan for two measurements with same τ_a and different α, IASBS site.

AMTD

6, 3317–3338, 2013

Polarized sun-photometer measurements for Zanjan atmosphere

A. Bayat et al.

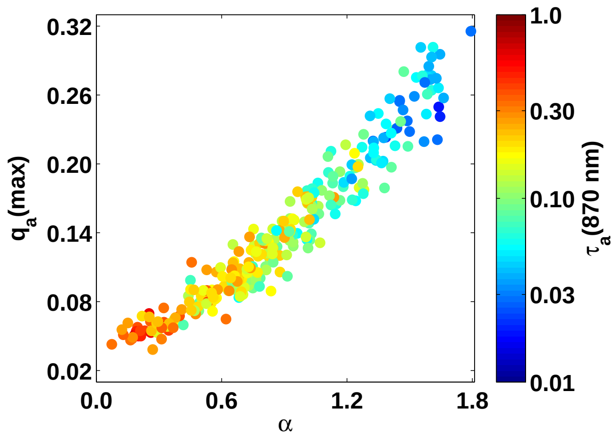

Fig. 3. Strong positive correlation between q_a(max) at 870 nm and α, colors are mapped to τ_a in logarithmic scale, January 2010 to December 2012, IASBS site.

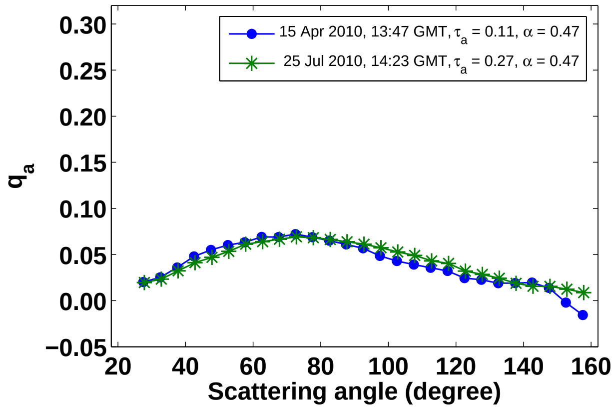

Fig. 4. Retrieved q_a at 870 nm in the atmosphere of Zanjan for two measurements with same α and different τ_a, IASBS site.

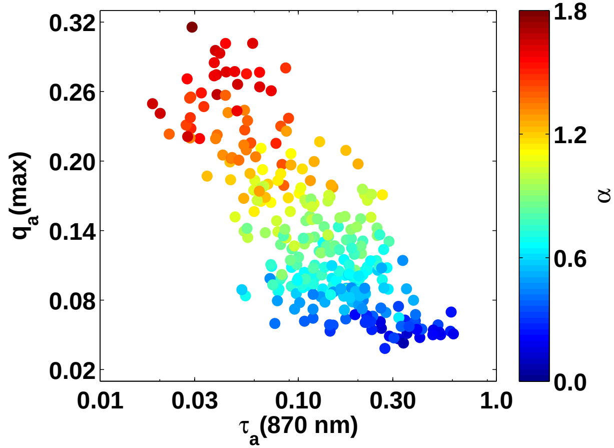

Fig. 5. Variations of q_a(max) versus τ_a(870 nm) in logarithmic scale, colors are mapped to α in linear scale, January 2010 to December 2012, IASBS site.

AMTD
6, 3317–3338, 2013

Polarized sun-photometer measurements for Zanjan atmosphere

A. Bayat et al.

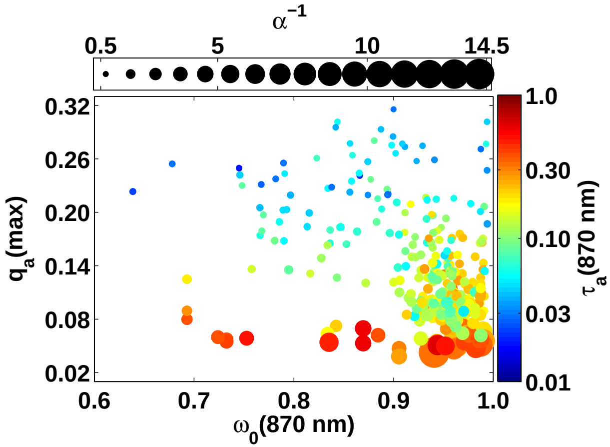

Fig. 6. Correlation between q_a(max) and ϖ_0 at 870 nm, colors are mapped to different values of τ_a. Diameter of each data point corresponds to α^{-1}.

AMTD
6, 3317–3338, 2013

Polarized sun-photometer measurements for Zanjan atmosphere

A. Bayat et al.

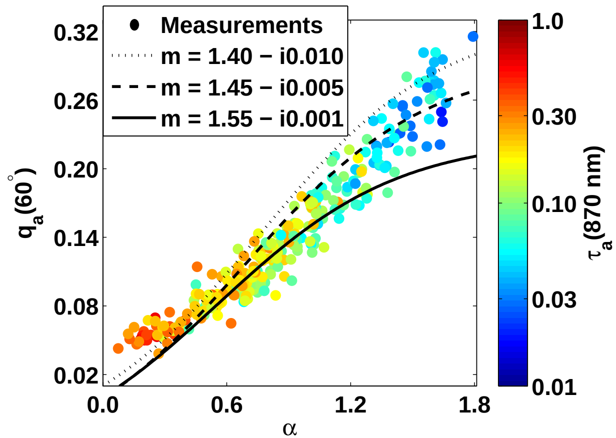

Fig. 7. $q_{\mathrm{a}}(60^\circ)$ versus α, for 305 retrieved data points (colored circles), lines calculated for three different presumed refractive indices based on Mie scattering theory.